Effective upwelling irradiance depths in turbid waters: a spectral analysis of origins and fate

Ronghua Ma,[1,*] Guangjia Jiang,[1] Hongtao Duan,[1] Luca Bracchini,[2] and Steven Loiselle[2]

[1]*Nanjing Institute of Geography and Limnology, Chinese Academy of Sciences, Nanjing, China*
[2]*University of Siena, CSGI, via Aldo Moro 1, Siena, Italy*
** rhma@niglas.ac.cn*

Abstract: The spectral distribution of upwelling and downwelling irradiance were used to estimate the effective upwelling irradiance depth as well as examine the angular distribution of the downwelling radiance. The effective upwelling depth was seen to undergo spectral "shifts" in wavelength maxima in relation to elevated particulate concentrations. Wavelengths of the UVA minimum and mid visible maximum depths were found to be shifted to higher wavelengths (red shifted) at high particulate concentrations, while expected minimums at chlorophyll and phycocyanin absorption peaks and in the NIR were shifted to lower wavelengths (blue shifted). By comparing upwelling and downwelling irradiance profiles, the wavelength limits of the asymptotic angular radiance distribution were found to correspond to the visible spectral domain (390 – 740 nm).

©2011 Optical Society of America

OCIS codes: (280.1415) Atmospheric and oceanic optics; (010.5620) Remote sensing and sensors.

References and links

1. D. G. Bowers, D. Evans, and D. N. Thomas, "Interpreting the colour of an estuary," Estuar. Coast. Shelf Sci. **59**(1), 13–20 (2004).
2. N. G. Jerlov, *Marine optics*, 2nd ed. Elsevier (1976).
3. N. K. Hojerslev, "Inherent and apparent optical properties of the Baltic. Report no.23," Institute of Physical Oceanography,University of Copenhagen (1977).
4. J. L. Mueller, and R. W. Austin, "Ocean Optics Protocols for SeaWiFS Validation, revision 1" (Maryland: Goddard Space Flight Center) (1995).
5. A. Islam, J. Gao, and W. Ahmad, "A composite DOP approach to excluding bottom reflectance in mapping water parameters of shallow coastal zones from TM imagery," Remote Sens. Environ. **92**(1), 40–51 (2004).
6. Z. Lee, K. L. Carder, C. D. Mobley, R. G. Steward, J. S. Patch, and B. Gentili, "Hyperspectral remote sensing for shallow waters. I. A semianalytical model," Appl. Opt. **37**(27), 6329–6338 (1998).
7. C. H. Chang, C.-C. Liu, and C. G. Wen, "Integrating semianalytical and genetic algorithms to retrieve the constituents of water bodies from remote sensing of ocean color," Opt. Express **15**(2), 252–265 (2007).
8. R. W. Preisendorfer, *Application of radiative transfer theory to light measurements in the sea," International Union of Geodesy and Geophysics Monographs* (1961).
9. H. R. Gordon, and A. Y. Morel, *Remote assessment of ocean colour for interpretation of satellite visible imagery: a review* in M. Bowman (Ed.), Lecture Notes on Coastal and Estuarine Studies (pp. 1–114), Springer-Verlag, New York, NY (1983).
10. L. Bracchini, A. M. Dattilo, V. Hull, S. A. Loiselle, A. Tognazzi, and C. Rossi, "Modelling Upwelling Irradiance using Secchi disk depth in lake ecosystems," J. Limnol. **68**, 83–91 (2009).
11. J. M. Sullivan, and M. S. Twardowski, "Angular shape of the oceanic particulate volume scattering function in the backward direction," Appl. Opt. **48**(35), 6811–6819 (2009).
12. J. T. O. Kirk, "The Upwelling Light Stream in Natural Waters," Limnol. Oceanogr. **34**(8), 1410–1425 (1989).
13. B. Q. Qin, *Lake Taihu, China: Dynamics and Environmental Change*, (Springer, Netherlands 2008).
14. R. Ma, H. Duan, X. Gu, and S. Zhang, "Detecting aquatic vegetation changes in Taihu Lake, China using multi-temporal satellite imagery," Sensors **8**(6), 3988–4005 (2008).
15. L. Guo, "Ecology. Doing battle with the green monster of Taihu Lake," Science **317**(5842), 1166 (2007).
16. H. Duan, R. Ma, X. Xu, F. Kong, S. Zhang, W. Kong, J. Hao, and L. Shang, "Two-decade reconstruction of algal blooms in China's Lake Taihu," Environ. Sci. Technol. **43**(10), 3522–3528 (2009).
17. T. Ohde, and H. Siegel, "Correction of bottom influence in ocean colour satellite images of shallow water areas of the Baltic Sea," Int. J. Remote Sens. **22**(2), 297–313 (2001).
18. J. D. Strickland, and T. R. Parsons, "A practical handbook of seawater analysis," Fishery Research Board, Canada (1972).

#141684 - $15.00 USD Received 25 Jan 2011; revised 28 Feb 2011; accepted 8 Mar 2011; published 30 Mar 2011
(C) 2011 OSA

19. R. Yan, F. Kong, and X. Han, "Analysis of the recruitment of the winter survival algae on the sediments of Lake Taihu by fluorometry," J. Lake. Sci. **16**, 163–168 (in Chinese with English abstract) (2004).
20. J. T. O. Kirk, *Light and Photosynthesis in Aquatic Ecosystems* (Cambridge Press, Cambridge 1994).
21. R. A. Maffione, "Theoretical developments on the optical properties of highly turbid waters and sea ice," Limnol. Oceanogr. **43**(1), 29–33 (1998).
22. M. Chami, D. McKee, E. Leymarie, and G. Khomenko, "Influence of the angular shape of the volume-scattering function and multiple scattering on remote sensing reflectance," Appl. Opt. **45**(36), 9210–9220 (2006).
23. M. Tedetti, B. Charriere, A. Bricaud, J. Para, P. Raimbault, and R. Sempéré, "Distribution of normalized water-leaving radiances at UV and visible wave bands in relation with chlorophyll a and colored detrital matter content in the southeast Pacific," J. Geophys. Res. **115**(C2), C02010 (2010).
24. M. M. Squires, L. F. W. Lesack, and D. Huebert, "The influence of water transparency on the distribution and abundance of macrophytes among lakes of the Mackenzie Delta, Western Canadian Arctic," Freshw. Biol. **47**(11), 2123–2135 (2002).
25. R. Ma, J. Tang, and J. Dai, "Bio-optical model with optimal parameter suitable for Taihu Lake in water colour remote sensing," Int. J. Remote Sens. **27**(19), 4305–4328 (2006).
26. B. J. Topliss, "Spectral variations in upwelling radiant intensity in turbid coastal waters," Estuar. Coast. Shelf Sci. **22**(4), 395–414 (1986).
27. N. Bergamino, S. Horion, S. Stenuite, Y. Cornet, S. Loiselle, P. D. Plisnier, and J. P. Descy, "Spatio-temporal dynamics of phytoplankton and primary production in Lake Tanganyika using a MODIS based bio-optical time series," Remote Sens. Environ. **114**(4), 772–780 (2010).
28. A. E. Hickman, S. Dutkiewicz, R. G. Williams, and M. J. Follows, "Modelling the effects of chromatic adaptation on phytoplankton community structure in the oligotrophic ocean," Mar. Ecol. Prog. Ser. **406**, 1–17 (2010).

1. Introduction

Upwelling irradiance plays a key role in primary productivity and radiative transfer, as well as determining the appearance of the water body [1]. As the upwelling irradiance is influenced by the angular distribution of the downwelling radiance and the optical properties of the water body, it has often been used to gain a better understanding of both and serves as the basis of remotely made observations of water quality in lakes, estuaries and the ocean. The maximum depth of the water column that influences the water leaving radiance can be defined as the "effective upwelling irradiance depth" ($z_{effective(\lambda)}$, m), below which the optical properties of the water body no longer influence the water leaving radiance. As in Jerlov's depth of penetration [2], the effective upwelling depth is strongly wavelength dependent. Similar to Secchi depth, the effective depth is closely related to the spectral attenuation properties of both the downwelling and upwelling light stream. For example, *Hojerslev* [3] estimated that lake bottom effects on the upwelling spectral signal can be considered insignificant when water depth is three times Secchi disk depth. *Mueller and Austin* [4] assumed that the bottom influence may be ignored when water depth is 2.5 times greater than attenuation length. However, $z_{effective(\lambda)}$ is strongly dependent on wavelength and on the angular properties of the downwelling and upwelling light field.

The relationship between $z_{effective(\lambda)}$ and the physical characteristics of the water body has important consequences on the interpretation of the water leaving radiance. If, at a specific wavelength, the effective depth is greater than the lake depth, the upwelling irradiance contains information about the spectral reflectance properties of the lake bottom, mediated by the optical properties of the intervening water layers [5]. Radiative-transfer models (e.g. Hydrolight) and semi-analytical models have had success in separating bottom and water column reflectances by using a typical particle phase function for specific water classes [6, 7]. If the water body is stratified and the effective depth is greater than the depth of the surface layer, upwelling irradiance will contain a depth-weighted exponential mean of the optical properties of the layers present.

Variations in the effective upwelling depth, like any apparent optical property, can be associated to changes in the inherent optical properties of the water body. Spatial and seasonal changes in these properties will modify the spectral attenuation of the upwelling or downwelling irradiance and therefore the effective upwelling depth.

The upwelling irradiance is the sum of upward traveling photons (< 90° with respect to the downward vertical direction). Typically, upwelling irradiance diminishes with depth in a

#141684 - $15.00 USD Received 25 Jan 2011; revised 28 Feb 2011; accepted 8 Mar 2011; published 30 Mar 2011
(C) 2011 OSA

similar manner to downwelling irradiance in a homogeneous medium (without optical stratification), following an exponential decay,

$$E_{u(\lambda,z)} = E_{u(\lambda,0)}\ e^{-K_{u(\lambda)}\ z} \quad (W\ m^{-2}) \tag{1}$$

where $E_{u(\lambda,z)}$ is the upward spectral irradiance at depth z, $K_{u(\lambda)}$ (m^{-1}) is the coefficient of exponential decay with depth and $E_{u(\lambda,0)}$ is the upwelling irradiance just below the surface. Equation (1) describes the spectral distribution of the upwelling irradiance at any depth in a vertically homogeneous medium, when no other sources of irradiance are significant (e.g. fluorescence, inelastic scattering). The term $E_{u(\lambda,0)}$ refers to the spectral distribution of the upwelling solar irradiance just below the surface in the same manner as $E_{d(\lambda,0)}$ is an estimate of downwelling irradiance just below the surface in the standard equation used to describe diffuse attenuation ($E_{d(\lambda,z)} = E_{d(\lambda,0)}\ e^{-K_{d(\lambda)}\ z}$). Both $E_{u(\lambda,0)}$ and $E_{d(\lambda,0)}$ provide information that is difficult to measure in normal field conditions (e.g. waves).

It should be noted that $K_{u(\lambda)}$ refers to the exponential reduction in upwelling irradiance with distance increasing downward, similar to $K_{d(\lambda)}$. In fact, the distribution of $K_{d(\lambda)}$ and $K_{u(\lambda)}$ are expected to closely correspond where the angular distribution of radiant intensity is asymptotic [8]. Often, the attenuation coefficient of upwelling irradiance is considered to be near or similar to $K_{d(\lambda)}$ [9, 10]. However, the angular distribution of the upward light stream is directed less towards the vertical and more towards the horizontal direction with respect to the downwelling irradiance [11]. This flattened radiance distribution results in a higher vertical attenuation, as the optical pathlength is increased. The expected value for the upwelling attenuation coefficient should be at least as large as $K_{u(\lambda)}$ or greater, depending on the relation between the angular distribution of the upwelling irradiance (e.g. backward scattering function [12]) and the cosine response of the spectroradiometer. To differentiate the upwelling irradiance attenuation coefficient from $K_{u(\lambda)}$, we use $\kappa_{(\lambda)}$, which is defined as the exponential change in transmittance ($T_{i(\lambda)}$) of upward scattered irradiance over a thin layer (Δz), $T_{i(\lambda)} = e^{-\kappa_{(\lambda)}\ \Delta z}$. Modeling upwelling irradiance using a Monte Carlo method, the ratio $\kappa_{(\lambda)}$ / $K_{d(\lambda)}$ has been found to range between 2.37 – 2.62, for a wide variety of optical conditions [12].

Having information on the upwelling and downwelling attenuation coefficients makes it possible to estimate the contribution of upwelling irradiance from any specific depth (e.g. $E_{u(\lambda,0.60\ m)}$) to the upwelling irradiance just below the surface ($E_{u(\lambda,0)}$)';

$$E_{u(\lambda,0)}' = E_{u(\lambda,0.60)}\ e^{-\kappa_{(\lambda)}\ 0.60} \quad (W\ m^{-2}). \tag{2}$$

where $E_{u(\lambda,0)}$' is the upwelling irradiance from $E_{u(\lambda,0.60)}$, which reaches the surface after attenuation in the intervening 0.60 m. As the upwelling irradiance at any depth can be determined from $K_{u(\lambda)}$ and $E_{u(\lambda,0)}$ (Eq. (1), the total upward irradiance measured below the surface ($E_{u(\lambda,0)}$) can then be determined by integrating the contribution from the surface to the effective upwelling depth, assuming optically homogeneous conditions in this layer:

$$E_{u(\lambda,0)} = \int_{z_{effective(\lambda)}}^{0} E_{u(\lambda,0)}\ e^{-K_{u(\lambda)}\ z}\ e^{-\kappa_{(\lambda)}\ z}\ dz \quad (W\ m^{-2}) \tag{3}$$

On the other hand, to determine the percentage ($P_{(\lambda)}$) of the total upwelling irradiance from depth z' in the upwelling irradiance measured just below the surface ($z=0$), it is possible to combine Eqs. (1) and 2 in the following manner;

$$P_{(\lambda)} = \frac{E_{u(\lambda,0)}'}{E_{u(\lambda,0)}} = \frac{E_{u(\lambda,z')}e^{-\kappa_{(\lambda)}\ z'}}{E_{u(\lambda,0)}} = \frac{E_{u(\lambda,0)}e^{-K_{u(\lambda)}\ z'}\ \ e^{-\kappa_{(\lambda)}\ z'}}{E_{u(\lambda,0)}}$$
$$P_{(\lambda)} = e^{-z'(K_{u(\lambda)}+\kappa_{(\lambda)})} \tag{4}$$

#141684 - $15.00 USD Received 25 Jan 2011; revised 28 Feb 2011; accepted 8 Mar 2011; published 30 Mar 2011
(C) 2011 OSA

Where $P_{(\lambda)}$ is the percentage of the upwelling irradiance from depth z' that contributes to the upwelling irradiance below the surface. If we define $z_{effective(\lambda)}$ as the depth above which 99% of the upwelling irradiance originates, then:

$$\ln(0.01) = -(K_{u(\lambda)} + \kappa_{(\lambda)})(z_{effective(\lambda)})$$
$$z_{effective(\lambda)} = \frac{4.61}{K_{u(\lambda)} + \kappa_{(\lambda)}} \quad (5)$$

The resulting effective depth of the upwelling irradiance (and water leaving radiance) assumes that optical conditions are vertically homogeneous (surface effects can be ignored), inelastic scattering is not significant and no other irradiance sources are present.

In the present study, we explore the spectral and spatial variability of the effective upwelling depth in Lake Taihu, where complex optical conditions are present but constant mixing creates vertically homogeneous conditions. We examine how inherent optical properties influence the effective depth, in particular how elevated particulate concentrations not only reduce $z_{effective(\lambda)}$.but also cause a spectral "shift".

2. Methods

Taihu Lake, with an area of 2,338 km^2 and a mean depth of 1.9 m, is a large shallow lake in the delta of Yangtze River. It is the third largest freshwater lake in China [13] and a major water resource for several important cities, including Suzhou (population 1.7 million) and Wuxi (population 2.2 million). Limited depth and long fetch create conditions of a well mixed water column where suspended sediments play an important part in the optical and nutrient conditions. Studies have shown that some areas of the lake have macrophyte growth, both submerged and emergent, and that this spatial distribution is dynamic [14]. Recent eutrophication has led to reoccurring algal blooms with strong interannual variations [15, 16]. In the present work, 100 sites were selected to examine the spatial heterogeneity of the effective upwelling depth and its relation to inherent optical properties. The measurements were made over 11 days in October 2008.

Profiles of upwelling and downwelling irradiance were made simultaneously using two TriOS spectroradiometers (RAMSES ACC VIS). Measurements were made every 0.30 meters to the lake bottom, usually at five depths (0.30 m, 0.60 m, 0.90 m, 1.20 m, 1.50 m) on the sunny side of the boat, under constant sky conditions and with wind speeds less than 2 m s^{-1}. Wavelength and energy calibrations were performed before measurements at each site, with a step of 5 nm between 350 nm and 950 nm. During immersion, measurements of downwelling and upwelling irradiance (256 ms integration time) were logged and processed using immersion offsets and calibration coefficients provided by the manufacturer in December 2007, so no correction factors were necessary [17]. Irradiance measurements were repeated five times at each depth under constant conditions. The average of the five irradiance measurements from 350 nm to 802 nm was used and values were interpolated in 3 nm increments to compensate for the slight wavelength offsets between spectrometers. All irradiance data with a signal to noise ratio of less than 10 was removed from the data set.

Where a sufficient number of irradiance measurement were available (≥ 4 depths), $K_{d(\lambda)}$, $K_{u(\lambda)}$, $E_{u(\lambda,0)}$ and $E_{d(\lambda,0)}$ were calculated using the LMFIT algorithm, a Levenberg-Marquardt nonlinear fitting method, within the Interactive Data Language program. The goodness of fit (R^2) was also determined for each wavelength and for each site. All estimates with a fitting above $p = 0.001$ ($R^2 < 0.95$) were removed from the data set.

Water samples were collected from the surface to a depth of 0.30 m using prerinsed standard 2 liter polyethylene bottles. The spectral absorbance by chromophoric dissolved organic matter (CDOM) was determined by manually filtering the water samples through a Whatman GF/F filter, and then through a 0.22-μm Millipore single use filter (Millipore, Malsheim, France). Absorbance spectra between 280 and 700 nm were acquired using a Shimadzu UV2401 spectrophotometer (Shimadzu Corp., Japan). Reference scans for instrument noise and bi-distilled water were also made. Absorbance, $A_{(\lambda)}$, was converted to

#141684 - $15.00 USD Received 25 Jan 2011; revised 28 Feb 2011; accepted 8 Mar 2011; published 30 Mar 2011
(C) 2011 OSA

absorption, $a_{CDOM(\lambda)}$, by $a_{CDOM(\lambda)} = \frac{2.303 \cdot A_{(\lambda)}}{r}$ where r is the pathlength in the cuvette. A baseline correction of the absorption at 700 nm was used to correct for scattering caused by fine particulates.

Suspended particulate matter (SPM) concentrations were determined gravimetrically from samples collected on pre-combusted and pre-weighed 47 mm GF/F filters, dried overnight at 95°C.

The concentrations of chlorophyll a (Chl-a) were determined spectrophotometrically after filtering using Whatman GF/F and then soaking in 90% ethanol in the dark for 4-6 hours. Samples were then heated to 80-90°C for 3-5 minutes. Absorbance of the extract was measured using a Shimadzu UV2401 spectrophotometer and concentrations determined following standard methods [18]. The concentrations of phycocyanin were determined after extraction with 0.05M pH 7.0 Tris buffer and using a Shimadzu UV2450 spectrofluorometer at an excitation wavelength at 620 nm and an emission wavelength at 647 nm [19].

3. Results

The downwelling and upwelling irradiance profiles showed a clear exponential decay with depth for all wavelengths considered (318 nm – 802 nm) and all sites (n=100) (Fig. 1a). Non linear fitting of the profiles showed a significantly good fit in 88 sites regarding the downwelling irradiance over the wavelength range (350 - 950 nm) and for 84 sites regarding upwelling irradiance ($R^2 > 0.95$, $p < 0.001$, $n \geq 4$). The spectral distributions of $K_{d\lambda}$ and $K_{u\lambda}$ showed the highest attenuation in the ultraviolet A (UVA 320 nm – 400 nm) and near infrared (NIR 700 – 800 nm) wavelengths. Small attenuation peaks occurred around 620 and 680 nm in many samples. A wide range of optical conditions were present in the lake. For clarity, we show the results of three sites (Fig. 1b) which represent an average attenuation (site 31), a site with high attenuation (site 12) and a site with low attenuation (site 78). The three sites are representative of the west, north and east parts of the lake, respectively.

The spectral distribution of the irradiance reflectance ($R_{(\lambda,z)} = E_{u(\lambda,z)} / E_{d(\lambda,z)}$) was determined by using the estimated upwelling and downwelling spectral irradiance just below the water surface, as well as the measured upwelling and downwelling irradiance from several depths (0.30, 0.60, 0.90, 1.20, 1.50 m). $R_{(\lambda,z)}$ is expected to remain constant with depth if; the effective depth is less than the mixing depth, optical conditions are vertically homogeneous and radiance distribution is asymptotic. The spectral reflectance distribution in the visible wavelengths did not vary significantly between depths (Fig. 2) for nearly all sites (ANOVA, significance level = 0.001). On the other hand, significant differences between irradiance reflectance occurred in the UVA and NIR.

Measurements of total suspended particulate matter (28.4 ± 23.7 g m^{-3}), chlorophyll a (24.8 ± 30.9 mg m^{-3}) and phycocyanin concentrations (2.0 ± 2.2 mg m^{-3}) show a wide range of values, indicating horizontally heterogeneous conditions. Elevated pigment concentrations indicate eutrophic conditions. CDOM absorption ($a_{CDOM(442)}$ = 0.82 ± 0.30 m^{-1}) was typical of inland waters [20].

#141684 - $15.00 USD Received 25 Jan 2011; revised 28 Feb 2011; accepted 8 Mar 2011; published 30 Mar 2011
(C) 2011 OSA

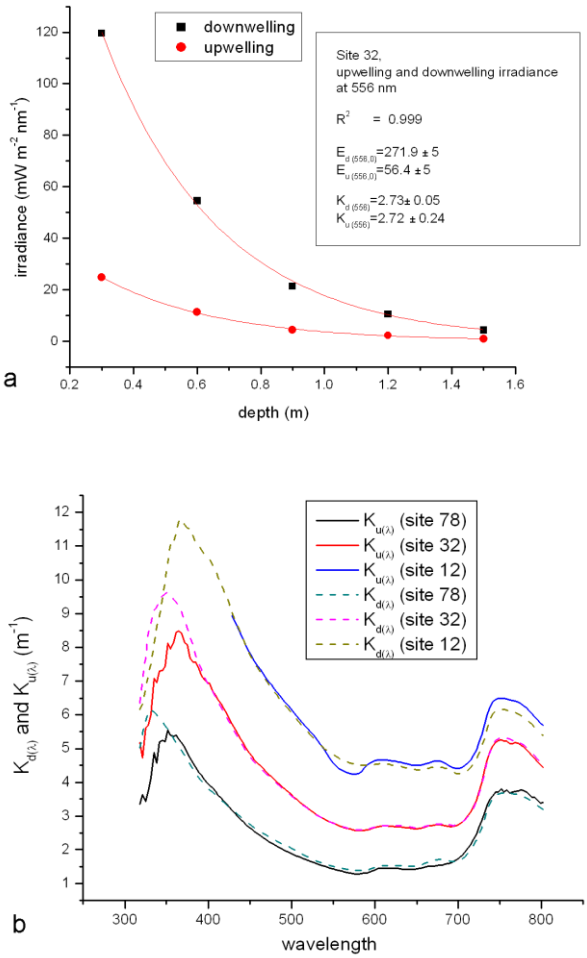

Fig. 1. a) Non linear fitting of the upwelling and downwelling irradiance at one site in Taihu Lake. b) Spectral distribution of vertical attenuation coefficients of upwelling and downwelling diffuse irradiance from three typical sites of Taihu Lake. Site 32, located on the eastern part of the lake has a spectral attenuation ($K_{d(\lambda)}$ and $K_{u(\lambda)}$) that is close to the average of all sites (at 500 nm). Site 12, located in the north part of the lake between Meiliang and Gonghu Bays has a higher attenuation (one standard deviation larger at 500 nm). Site 78, located on the western part of the lake is characterized by lower attenuation (close to one standard deviation smaller at 500 nm).

#141684 - $15.00 USD Received 25 Jan 2011; revised 28 Feb 2011; accepted 8 Mar 2011; published 30 Mar 2011
(C) 2011 OSA

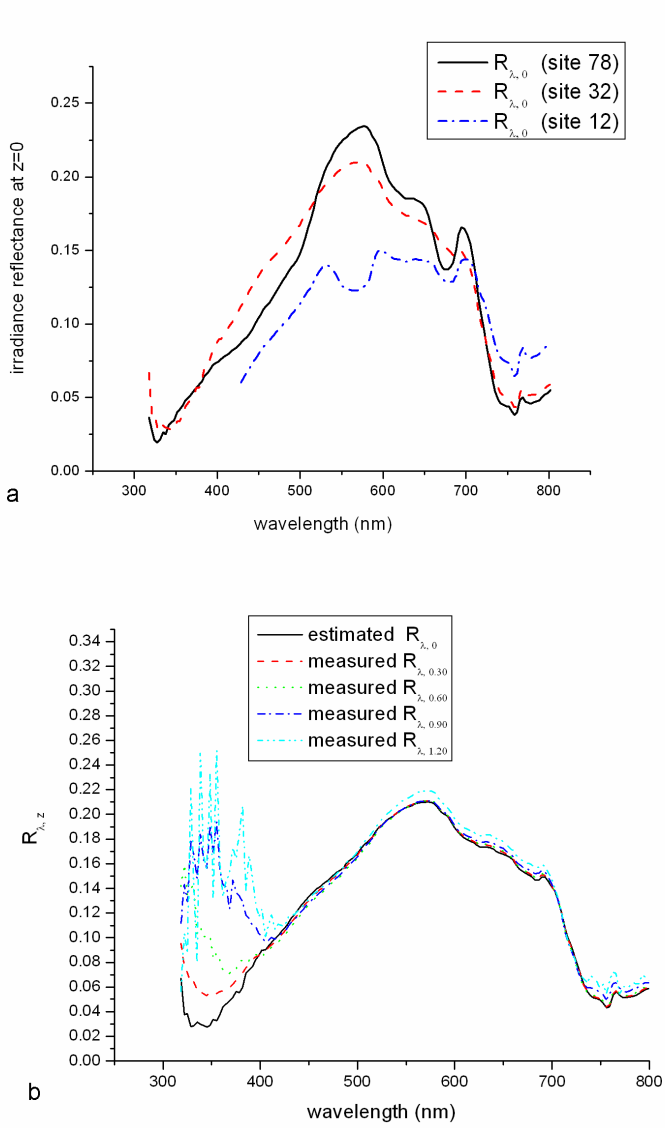

Fig. 2. a) The spectral irradiance reflectance ($R_{(\lambda)}$) from three sites in Taihu Lake, b) the spectral irradiance reflectance from different depths from site 32 in Taihu Lake, a site with average attenuation.

4. Discussion and conclusions

The estimation of $K_{d(\lambda)}$, $K_{u(\lambda)}$, $E_{d(\lambda,0)}$ and $E_{u(\lambda,0)}$ allowed for the determination of the spectral distribution of upwelling and downwelling irradiance at any depth and at any site throughout the lake. To examine the fate of upwelling irradiance from any depth and its contribution to the upwelling irradiance below the surface, we used $\kappa_{(\lambda)} = 2.5\ K_{d(\lambda)}$, as no direct information on the angular distribution of upwelling radiance was available and the lake was characterized by high particulate concentrations.

4.1 Angular distribution of radiance and verification of asymptotic conditions

The determination of $z_{effective(\lambda)}$.will depend upon the angular distribution of radiance. In ocean waters, the asymptotic region can initiate after many meters. However, in turbid waters

#141684 - $15.00 USD Received 25 Jan 2011; revised 28 Feb 2011; accepted 8 Mar 2011; published 30 Mar 2011
(C) 2011 OSA

(shallow lakes, estuaries and rivers), radiance distribution approaches an asymptotic shape quickly as scattering dominates absorption, in particular in the visible spectrum [21, 22].

The depth at which asymptotic attenuation begins will be both wavelength and ecosystem dependent and generally occur first in the visible wavelengths, and later in the UVA and NIR. In the UVA, absorption increases exponentially, making it comparable with scattering. Likewise, absorption rises in the NIR and can contribute significantly to overall attenuation. This depth can be examined by comparing the spectral irradiance profiles. At the wavelengths where an radiance distribution is asymptotic, the exponential coefficients of the change of irradiance with depth should have similar values. Therefore a comparison of $K_{u\lambda}$ and $K_{d\lambda}$ allows for the identification of the wavelength limits of our hypothesis of asymptotic conditions.

Similarly, irradiance reflectance ($R_{(\lambda,z)}$) should be independent of depth in the asymptotic region. Wavelengths where $R_{(\lambda,z)}$ changes with depth indicate that the shape of angular distribution is not constant, or in general, that optical conditions are not vertically homogeneous. This can be important where cyanobacteria are present and can form layers of elevated biomass concentrations at specific depths.

In the present data set, both $K_{u(\lambda)}/ K_{d(\lambda)}$ and $R_{(\lambda,z_1)} / R_{(\lambda,z_2)}$ are nearly unity throughout the visible wavelengths. This indicates that the water column is well mixed and no stratification of optically active components is present. However, in the UVA and NIR, irradiance reflection changes with depth in many sites. Likewise, values of $K_{u\lambda}$ and $K_{d\lambda}$ are significantly different in the UVA and NIR (Figs. 1 and 2). On average, the transition between similar values ($K_{u(\lambda)}/ K_{d(\lambda)} <1.05$) and dissimilar values ($K_{u(\lambda)}/ K_{d(\lambda)} >1.05$) occurs at 390 nm and 740 nm. However, this transition varies from site to site. The poor relationship between $K_{d(\lambda)}$ and $K_{u(\lambda)}$ at wavelengths in the UVA and NIR indicates that asymptotic conditions cannot be assumed. Thus, the comparison of irradiance profiles provides important information on the angular distribution of the light field and allows for the definition of wavelength limits in the determination of $z_{effective(\lambda)}$. These wavelength limits should be taken into consideration when relationships between upwelling and downwelling irradiance are used to explore the origin of the water leaving radiance.

4.2 Effective upwelling depth in Taihu Lake

The contribution of the upwelling irradiance from different depths to the total upwelling irradiance just below the surface varied significantly between sites (Fig. 3a). More than 20% of the upwelling irradiance at the surface of site 78 can be associated to that which was present at 0.30 m, in the wavelength interval between 546 nm and 656 nm. At site 12, on the other hand, barely 1% of the upwelling irradiance at the surface originated at or below 0.30 m. At this site, elevated attenuation limited the contribution of upwelling irradiance to depths closer to the surface. The measurements at site 32, which represents an average attenuation for the lake, indicated that more than 5% of the upwelling irradiance in the mid visible wavelengths originated at or below 0.30 meters.

#141684 - $15.00 USD Received 25 Jan 2011; revised 28 Feb 2011; accepted 8 Mar 2011; published 30 Mar 2011
(C) 2011 OSA

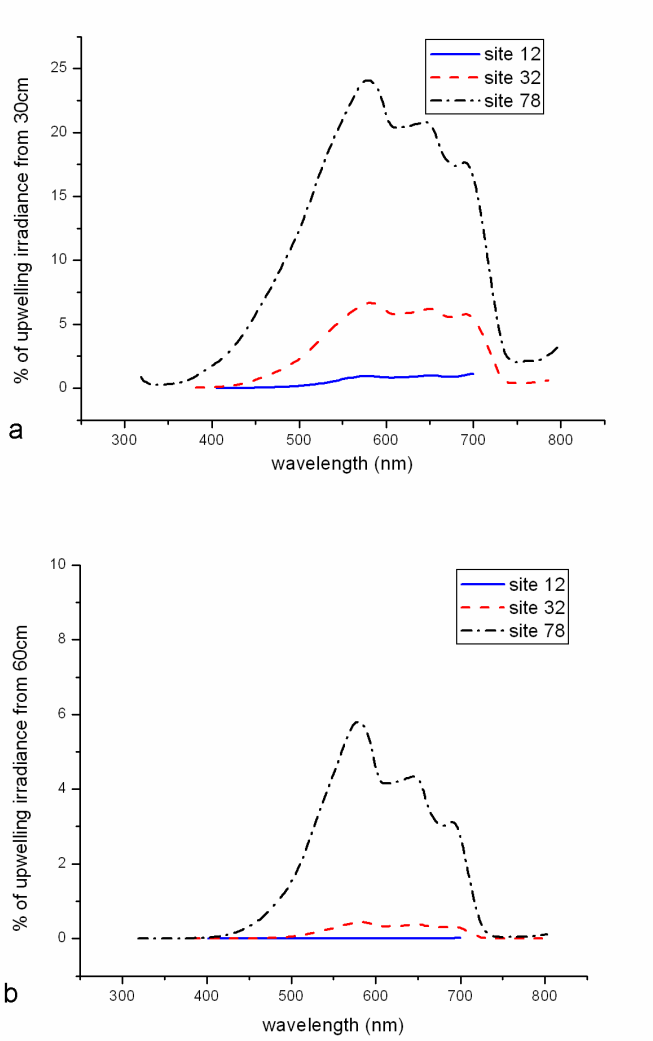

Fig. 3. The percentage of total upwelling irradiance measured just below the water's surface which originating at or below 0.30 m (a) and 0.60 m (b).

From greater depths, the contribution of upwelling irradiance was necessarily less, as upwelling irradiance diminishes with distance from the surface. The contribution of the upwelling irradiance from 0.60 m was significant (> 1%) for 31% of all sites at 586 nm (Fig. 3b). Only 12% of the measurement sites had significant contributions from a depth of 1 m. to upwelling irradiance at the surface (λ = 586 nm). From 1.5 m., this percentage falls to less than 5%.

The origin of the upwelling irradiance at each wavelength and at each site depends on the effective upwelling depth and the lake depth. Using the three typical sites described previously, the spectral distribution of $z_{effective(\lambda)}$ had a clear maximum in the mid-visible wavelengths, with minimums in both the UVA and NIR regions (Fig. 4). The elevated $z_{effective(\lambda)}$ estimated for site 78 indicates that surface upwelling irradiance carried information from depths up to 1.0 m in the visible. Upwelling irradiance at site 32 contained information on the optical properties of the lake from no deeper than 0.50 m in the mid-visible and a minimum effective depth of 0.18 m at 390 nm. Site 12, with a high attenuation, had a maximum $z_{effective(\lambda)}$ of 0.32 m.

#141684 - $15.00 USD Received 25 Jan 2011; revised 28 Feb 2011; accepted 8 Mar 2011; published 30 Mar 2011
(C) 2011 OSA

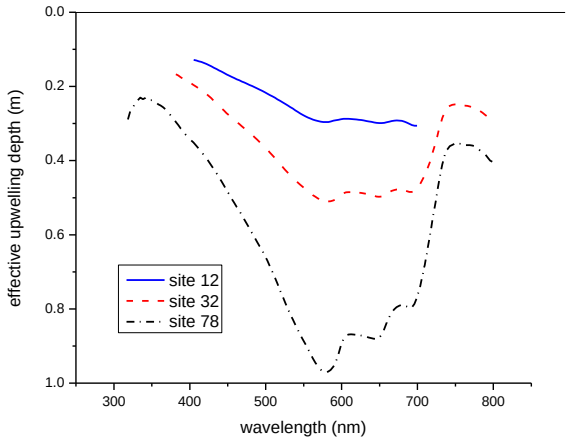

Fig. 4. Spectral distribution of effective upwelling depth from three sites in Taihu Lake. Water surface (dashed line) also shown. The spectral range of asymptotic radiance differ between sites, site 12 (400 – 701 nm), site 32 (380 – 790 nm), site 78 (320 – 795 nm).

The effective upwelling depth can be used to identify the portion of the water column which influences the water leaving radiance in specific wavebands typically present on passive optical sensors. A spatial distribution of this apparent optical property (Fig. 5) shows that, for upwelling irradiance at 412 nm, $z_{effective(\lambda)}$is less than 0.40 m for most of the lake, indicating that estimates of inherent optical properties using wavebands centered on this wavelength are dominated by the near surface waters [23]. Effective upwelling depths at 559 nm and 683 nm are larger, reaching 0.70 m in most of the lake. The eastern part of the lake had the greatest $z_{effective(\lambda)}$, with some areas reaching over 1.40 meters. If a comparison with lake depth is made, the effective depth in much of the eastern part reaches to 60% of the lake depth, whereas those to the west are often less than 20%. Using this same information, it is possible to determine that upwelling irradiance from the lake bottom did not contribute significantly to the subsurface upwelling irradiance at any site. However, submerged macrophytes, dominated by *Potamogeton malaianus* cover the eastern area of the lake and extend into the water column [14]. When this vegetation reaches the effective depth, related reflectance will influence the upwelling and water leaving reflectance. It should be noted that submerged vegetation has both direct and indirect influences on reflected irradiance. For vegetation that does not reach the effective depth, but does increase particulate deposition (reducing particulate related absorption and scattering), a reduction in the water leaving radiance may occur, compared to areas without submerged vegetation [24]. The higher $z_{effective(\lambda)}$ in the south east part of the lake (Fig. 5) agree with previous optical regionalizations of the lake [25].

#141684 - $15.00 USD Received 25 Jan 2011; revised 28 Feb 2011; accepted 8 Mar 2011; published 30 Mar 2011
(C) 2011 OSA

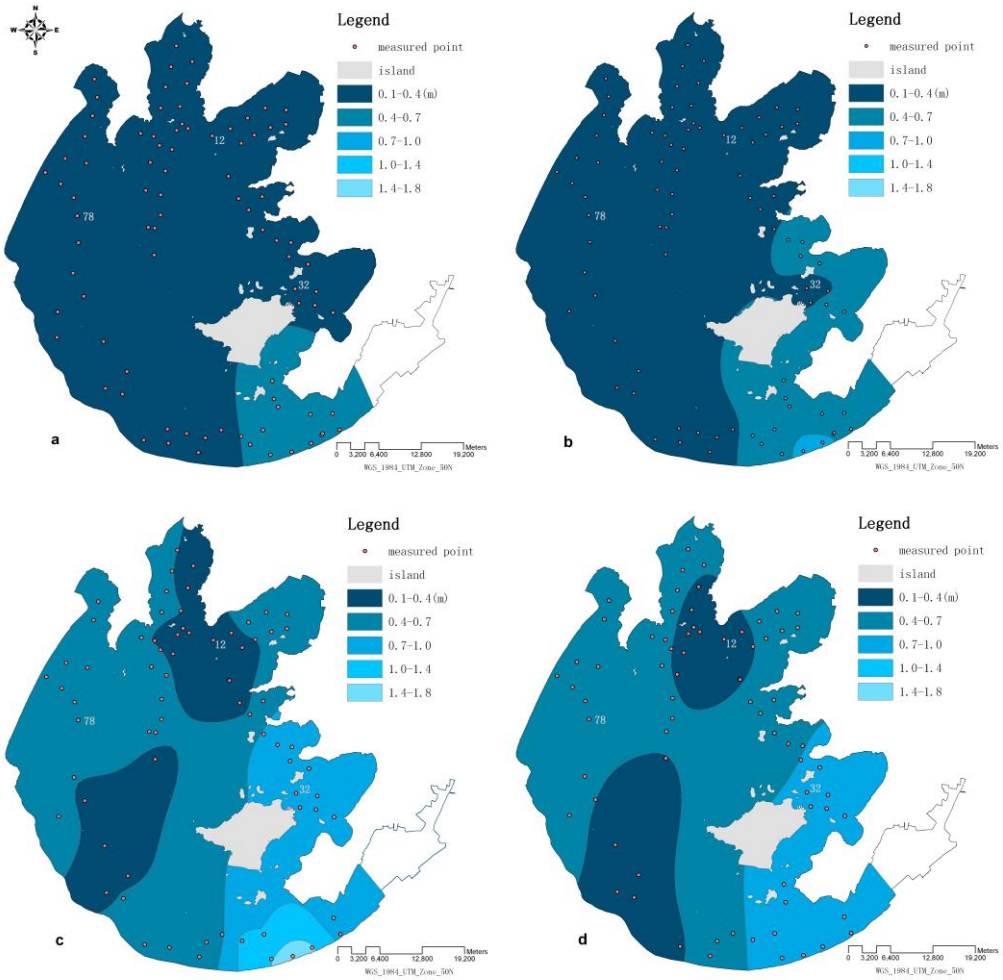

Fig. 5. Effective depth for Taihu Lake in October 2008 at a) 412 nm, b) 442 nm, c) 559 nm, d) 683 nm. Sample sites are indicated by a red circle, sites 12, 32 and 78 indicated. It should be noted that it was not possible to make measurements in the shallow bay in the southeast part of the lake (in white).

4.3 The effective upwelling depth and biogeochemical parameters

The spectral distribution of the effective upwelling depth has a characteristic shape for all sites, two minimum values (in the UVA and NIR) and a maximum in the mid-visible wavelengths, while many sites showed small negative peaks at 620 nm and 676 nm. By comparing these values of maxima and minima to the optical properties of the lake samples, it is possible to identify relationships between them (Table 1). An elevated and significant correlation between all maxima/minima and particulate concentrations was observed (critical value for Pearson, two tailed test, n= 84, p = 0.01, r >0.30). No significant correlation with CDOM absorption (at 442 nm) was present, while low correlations with CDOM absorption at 350 nm were observed. Low but significant correlations between pigment concentrations and peaks at 620 nm and 680 nm occurred. It should be noted that the concentrations of particulates, chlorophyll a and phycocyanin were all correlated (n = 97, r > 0.50).

A closer look at the wavelength distribution of the $z_{effective(\lambda)}$ indicates that the position of the maxima and minima (λ_{max} or λ_{min}) was not fixed but fell into a range of values. The wavelength of the $z_{effective(\lambda)}$ maximum in the visible wavelengths ranged from 570 nm to 590

#141684 - $15.00 USD Received 25 Jan 2011; revised 28 Feb 2011; accepted 8 Mar 2011; published 30 Mar 2011
(C) 2011 OSA

nm. The expected peaks in $z_{effective(\lambda)}$ around 620 nm and 680 nm had ranges of 606 – 629 nm and 662 – 680 nm, respectively. The expected minimums in the UVA and NIR demonstrated significant shifts in peak position, 330 - 390 nm and 750 – 769 nm, respectively. To better understand the causes of this spectral shift, we compared the wavelength of each peak with the optical properties of the lake samples (Table 1). An elevated correlation between the position of all maxima/minima and particulate concentrations was observed.

While the negative correlation between peak height and particulate concentrations is to be expected (an increase in particulate associated absorption and scattering should decrease in the effective depth), the strong correlation between particulate concentrations and the position (wavelength) of the maxima/minima is unexpected. The position of the UVA minimum and the mid visible maximum were both found to be shifted to higher wavelengths (red shifted) at high particulate concentrations, while expected minimums at 620 nm, 680 nm and in the NIR were shifted to lower wavelengths (blue shifted). Red shifts in the upwelling maxima have been reported for turbid waters [26], but shifts for both maxima and minima were not found in the current literature.

Spectral shifts in $z_{effective(\lambda)}$ may be important in the interpretation of remotely observed radiances from turbid waters. Knowing that such shifts occur allows for a more informed analysis of potential bottom effects. Furthermore, shifts in $z_{effective(\lambda)}$ maxima/minima are related to spectral variations in diffuse attenuation coefficients, which are basic parameters (e.g. K_{490}) in many ocean colour algorithms [27]. It should also be considered that spectral shifts in diffuse attenuation have been shown to influence species selection, for example in the vertical structuring of pico-phytoplankton in the ocean [28]. More research is necessary to determine whether spectral shifts are sufficient to influence the horizontal species distribution in shallow lakes. It should be noted that upwelling irradiance constitutes up to 21% of the total irradiance available (at 675 nm) in the Taihu Lake waters.

Table 1. Pearson correlation coefficients (r) between peaks (wavelength, peak value) of effective upwelling depth and CDOM absorption, total suspended particulate matter concentrations, chlorophyll a and phycocyanin concentrations.

	$a_{CDOM442}$ (m^{-1})	$a_{CDOM352}$ (m^{-1})	SPM ($g\ m^{-3}$)	Chl a ($mg\ m^{-3}$)	Phycocyanin ($mg\ m^{-3}$)
Peak values (m)					
min in UVA	–0.27	–0.44*	–0.72*	–0.46*	–0.40*
Max	–0.20	–0.31*	–0.49*	–0.31*	–0.38*
min 620	0.04	–0.20	–0.43*	–0.28	–0.34*
min 680	–0.17	–0.29	–0.77*	–0.44*	–0.44*
minNIR	–0.07	–0.10	–0.37*	–0.24	–0.29
Peak position (nm)					
λ of min UVA	0.23	0.45*	0.89*	0.65*	0.57*
λ of max depth	0.16	0.29	0.63*	0.24	0.19
λ of min ~620 nm	–0.18	–0.40*	–0.63*	–0.29	–0.32*
λ of min ~680 nm	–0.21	–0.42*	–0.65*	–0.52*	–0.40*
λ of min NIR	–0.28	–0.33*	–0.46*	–0.28	–0.22
* Significant correlations ($n = 84$, $p < 0.01$)					

Acknowledgments

We would like to acknowledge the financial support provided by the Knowledge Innovation Program of the Chinese Academy of Sciences (No.KZCX2-YW-QN311), the National Natural Science Foundation of China (No.40801137 and No.40871168), and the Chinese Academy of Sciences Visiting Professorships for Senior International Scientists (Grant number 2009Z2-8).